J Therm Anal Calorim (2012) 110:405–412
DOI 10.1007/s10973-012-2433-0

Structure of white cement mortars with high content of marble powder

V. Stoyanov · B. Kostova · V. Petkova · Y. Pelovski

CEEC-TAC1 Conference Special Chapter

Abstract In this study, three types of cementitious composites based on (i) white Portland cement and sand (cement-to-aggregate 1:3, and water-to-cement 0.50), (ii) white Portland cement and marble powder (cement-to-aggregate 1:2, and water-to-cement 0.60), and (iii) white Portland cement and marble powder with polycarboxylate-based admixture (HRWR) (cement-to-aggregate 1:2, and water-to-cement 0.40 + HRWR) were studied. Their states after 28 and 120 days of water curing were evaluated by measurement of physical–mechanical properties, such as density, compressive strength and porosity. Thermal analysis, X-ray diffraction analysis and scanning electron microscopy were used to identify the crystal phases and their morphology. The experimental data show that the white cement mortars with higher water content exhibit larder variety of newly formed phases, like hydration products of the C–S–H type. The structure of mortars with polycarboxylate-based admixture is so dense that there is no possibility of crystal hydrates development at late curing ages. The use of marble as filler leads to a partial inclusion of carbonate ions in the newly formed hydrated phases (carbo-aluminates).

Keywords White Portland cement · Self-compacting concrete · Cement hydration · Marble filler · Polycarboxylate-based admixture

V. Stoyanov
Institute of Mechanics, Bulgarian Academy of Sciences, Acad. G. Bonchev Str., Bl. 4, 1113 Sofia, Bulgaria

V. Stoyanov
European Polytechnical University, Sv. Sv. Kiril i Metodiy Str. 23, 2300 Pernik, Bulgaria

B. Kostova
Department "Earth and Environmental Sciences", New Bulgarian University, 21 Montevideo Str, 1618 Sofia, Bulgaria

V. Petkova (✉)
Institute of Mineralogy and Crystallography, Bulgarian Academy of Sciences, Acad. G. Bonchev Str., Bl. 107, 1113 Sofia, Bulgaria
e-mail: vilmapetkova@gmail.com

Y. Pelovski
University of Chemical Technology and Metallurgy, 8 Kl. Ohridski Str, 1756 Sofia, Bulgaria

Introduction

The decorative cement mortars and concretes are an artificial imitation of the natural stones. The main advantage of these artificial stones is their better workability, but the durability and stability are their key disadvantages. To achieve a good aesthetic surface of decorative composites, which allows for their multilateral application (decorative stamp concrete, pots, balustrade, ornamental stones, restoration of architectural monuments, decoration of facades, fences, terraces, etc.), it is necessary to use white Portland cement and white or colour aggregates [1–4]. The limitations of the used cement, surface properties of aggregates and the necessity of greater quantity of water suggest large differences in the formed structure of these cement compositions, compared with conventional ones [1, 5]. A great opportunity in decorative cement mortars is to use the polycarboxylate-based admixtures, which causes steric repulsion of fine particles and marble filler (of a 1:2 mass ratio) [5, 6]. Owing to superior water-reduction capabilities of these admixtures, the workability of the fresh mixes is improved, but it is possible to increase the amount of fine particles [6–8]. As a result, the hardened mortars are

characterized with high early-strength, smooth surfaces and dense structure [7, 9].

This research aims to study the phases, formed in different types of decorative cement composites. The accent of this study is on the phase formation at the later stages of curing, especially when polycarboxylate-based admixture is used.

Experimental

The chemical composition of the used white Portland cement CEM I 52.5 N, produced by Devnya Cement (Bulgaria), is (in wt%): SiO_2—24.3; Al_2O_3—2.1; Fe_2O_3—0.2; CaO—68.3; MgO—0.3; Na_2O—0.13; K_2O—0.02; and Free lime—1.9. The mineral composition of the white cement was calculated using Bogue's method based on the chemical compositions (in wt%): C_3S—72.13; C_2S—15.28; C_3A—5.23; C_4AF—0.61. The other properties of white cement are total mass losses at 1,000 °C–5.17 %, Blaine specific surface—4446 cm^2/g; 28-days compressive strength—56.1 N/mm^2; water demand—30 %, soundness (Le Chatelier)—1.0 mm; whiteness—80.1 %.

The mortars were prepared using two types of aggregates. For the reference sample, clean washed and dried river sand was used. The properties of sand are fineness modulus—2.7 (EN 12620:2002 + A1:2008/HA:2008), and shape index—4.6 % (EN 933–4:2008), i.e. spheroid particles, over 85.0 % content of SiO_2. The studied samples were prepared with marble powder, produced by AIAS S.A. White marble products (Greece) have the chemical composition (in wt%): $CO_2 + H_2O$—45.7; SiO_2—0.12; Al_2O_3—0.38; Fe_2O_3—0.14; CaO—32.9; MgO—20.0; Na_2O—0.05; K_2O—0.19; MnO—0.01. The decarbonization at 1,000 °C of this aggregate was divided to two stages (DTA peaks—806.6 and 821.2 °C) with a total mass loss of about 45 % and, thus the mineral composition is dolomite/Mg-rich calcite. The polydispersity of aggregate is maximal size of grains—2 mm; grains with sizes <0.125 mm—50.0 wt%; grains with sizes <0.063 mm—35.0 wt%.

The polycarboxylate-based high range water reducer (HRWR) Sika ViscoCrete 5-800 was used and its dosage was 2.0 % by weight of white cement. This HRWR was chloride-free, soluble in water, without any retarding effects, having a density of 1.07 g/cm^3 (at 20 °C).

The experiments were carried out with three types of cement composites, are shown in Table 1. All the samples were mixed with distilled water.

The composition of the reference sample A satisfied the requirements, as described in EN 196-1 (Sect. 6) [10] for determination of the compressive strength of cement. The mortars were prepared by mechanical mixing, and they were compacted in moulds using a standard jolting apparatus. The samples of series B were prepared according to the EN 196-1, with the same cement-to-aggregate ratio and with the maximum possible amount of water, where the sedimentation or segregation borders were not observed 10 min after mixing. The composition of samples C was determined by optimization to achieve high-quality smooth surfaces of the hardened samples [11]. This procedure was applied to the data obtained from experimental tests (D-optimal plan with constant cement-to-aggregate ratio). The samples C were prepared by mixing procedure, according to the EN 196-1, with prolonged time of homogenization at high speed (to obtain self-levelling behaviour or 120 s). The samples B and C were moulded without any compacting treatment.

Table 1 Codes and compositions of the samples

Sample	Aggregate	Ratios		
		Cement-to-aggregate	Water-to-cement	Water-to-powder[a]
A	Sand	1:3	0.50	0.500
B	Marble powder	1:2	0.60	0.353
C	Marble powder	1:2	0.40 + HRWR	0.235

[a] All particles with sizes below 125 μm

After casting, the specimens (6 prisms, 40 × 40 × 160 mm) were stored in the moulds for 1 day in a moist atmosphere (>95 % RH and 20 °C). Then the demoulded specimens were stored under water (20 °C) until strength testing (28 and 120 days).

Experimental methods

The bulk density after immersion and adsorption after immersion were measured according ASTM C642: 2006 [12]. Owing to the different bulk densities of the samples, the values of adsorption were adjusted to comparable values. The compressive strengths at 28 and 120 days of water curing were measured according EN 196-1:2006 [10].

Broken parts of sample with weight of 2.0 ± 0.3 mg were used to measure the porosity by mercury intrusion porosimetry method using Carlo Erba, Porosimeter Mod. 1520, pressure range 1–150 atm corresponding to pore size range 50–15,000 nm. The XRD patterns were performed on X-ray powder diffractometer D2 Phaser BrukerAXS, CuKα radiation ($\lambda = 0.15418$ nm) (operating at 30 kV, 10 mA) from 5 to 70°2θ with a step of 0.05° (ground sample with weight—1.0 ± 0.1 mg and particle sizes below 0.075 mm). The microstructures were observed on Philips PH Model 515, regime of secondary electron emission. The fracture fragments of the samples with approximately flat surface of about 10 × 10 mm was dried for 12 h at 60 ± 5 °C, and then were coated with a thin layer of gold.

Results and analysis

Physical-mechanical properties

The physical–mechanical properties of the studied samples are shown in Table 2. The 28-day compressive strength of conventional cement mortar A is comparable to that given by the factory, which indicates that the sand used is similar to CEN Standard sand, EN196-1. The compressive strength increases by 7.6 % by the 120th day, because of the filling of porous space with newly formed hydrates (the pore volume increases by 6.8 %).

The values for the measured parameters are evidence of thin structure of the hardened samples B, which are characterized by high water-to-cement ratio. The presence of fine particles decreases the water-to-powder ratio, but does not increase the density of the structure. The prolonged water curing increases the compressive strength by 14.3 %, or whichever is greater than the decrease of total pore volume by 9.3 %. The same pattern is observed for samples C, where the increase of compressive strength (17.9 %) is greater than the decrease of the total volume of pores (9.8 %) with sizes in the studied range.

The use of HRWR allows a reduction of water by 33.3 %, which increases the bulk density and adsorption; the latter is commensurate with the decrease of water amount. The formed structure of samples C is very dense, which is detected when comparing the pure volume of samples, recalculated from the measured value of pore volume and bulk density after immersion, i.e. at 28 days of curing: 21.1 mm^3/cm^3 (Sample A); 17.6 mm^3/cm^3 (Sample C); 30.0 mm^3/cm^3 (Sample B).

However, these samples have an open porosity, which allows for penetration of the water through pores and capillaries, causing slow continuous hydration of cement grains. Another characteristic pattern of data is the high adsorption of samples with marble powder as aggregate (samples 2 and 3), which can be explained by the high water absorption capacity of the fine marble particles.

XRD

The X-ray powder diffraction was used to check previously obtained results as well as to better evaluate the investigated samples. The obtained results from XRD analyses are shown in Fig. 1a–c and in Table 3.

The XRD analysis (Table 3) shows the presence of two groups of minerals in the studied samples: (i) relict minerals from the initial composition: belite, plagioclase, Mg-rich calcite for the samples A, B and C, quartz—sample A, dolomite—samples B and C and (ii) newly formed minerals: portlandite (all samples), mono- (B120 and C120), and hemicarboaluminate (B28 and C28), thaumasite (A28 and A120), ettringite (all samples), hillebrandite (B28, B120 and C28) and xonotlite (B28, B120 and C28).

The existence of relicts (belite and plagioclase) is caused by an unfinished process of cement hydration, due to the insufficiency of water. This could be explained with both low pore volume (Table 2) and higher silicate component in the system (Tables 1, 3). This behaviour could be explained with the presence of HRWR.

The new hydrate minerals are identified, and they are characterized by low content of crystallization water. The portlandite, which is formed immediately after contact of the cement with the water, persists in all the samples at different ages of curing.

The identification of mono- (B120 and C120), and hemicarboaluminate (B28) shows the contribution of carbonate ions introduced in the system from the aggregate—dolomitic marble, i.e. dolomite and Mg-rich calcite. The sulphate ions are involved in the formation of thaumasite and ettringite. Thaumasite and hemicarboaluminate crystallize in the initial days of water curing, while ettringite and monocarboaluminate after prolonged time of water curing. The samples B and C are characterized by high content of carbonate ions [13], which causes the isomorphic substitution in thaumasite [14, 15] and ettringite [16] during their hydration, which occurs in the following reactions:

$$6Ca^{2+} + 2AlO_2^- + 3CO_3^{2-} + 3SO_4^{2-} + 6OH^- + 26H_2O \rightarrow 3Ca(OH)_2{\cdot}3CaCO_3 \cdot Al_2(SO_4)_3{\cdot}26H_2O \quad (1)$$

$$3Ca^{2+} + HSiO_3^- + CO_3^{2-} + SO_4^{2-} + OH^- + 14H_2O \rightarrow 3Ca(OH)_2{\cdot}Si(SO_4 \cdot CO_3) \cdot 12H_2O \quad (2)$$

The content of calcium silicate hydrates (C–S–H) are mono-, and hemicarboaluminate, thaumasite, ettringite, hillebrandite and xonotlite. The largest diversity of C–S–H

Table 2 Physico-mechanical properties of the samples

Sample	Bulk density after immersion	Adsorption after immersion	Compressive strength		Pore volume	
			28 days	120 days	28 days	120 days
	kg m^{-3}	mm^3 cm^{-3}	N mm^{-2}	N mm^{-2}	mm^3 g^{-1}	mm^3 g^{-1}
A	2126	173.8	56.3	60.6	44.98	41.91
B	2158	258.5	53.8	61.5	64.66	58.69
C	2348	192.5	90.1	106.2	41.30	37.26

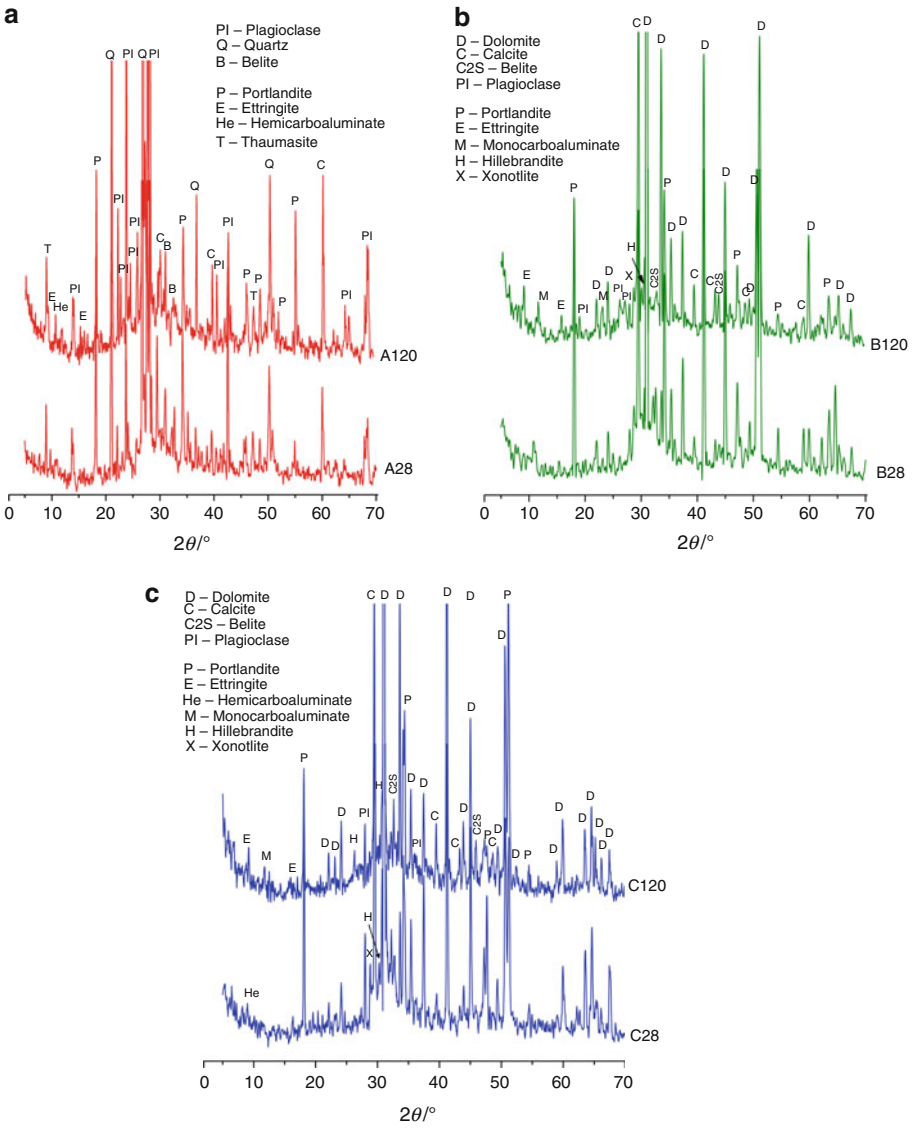

Fig. 1 **a** X-Ray patterns of samples A28 and A120 (28 and 120 days of water curing). **b** X-Ray patterns of samples B28 and B120 (28 and 120 days of water curing). **c** X-Ray patterns of samples C28 and C120 (28 and 120 days of water curing)

is found in sample B120, where the conditions for early- and late-hydration are the most favourable.

SEM

The surface structures of the studied samples are shown in Fig. 2a. The micrographs indicate stable and dense structures, even at 28 days of curing, and so there are no empty spaces for the growth of new minerals. The C–S–H gel forms fine-grained crystal aggregate, probably with structural parameters under the limit of XRD detection. In addition, on these micrographs areas with self-desiccation, drying cracks can be seen.

Figure 2b shows the surface morphology of the samples, obtained for areas with empty spaces—air bubbles involved in structure during sample preparation. Due to wall effects, different cement-to-water ratio and empty space these areas are filled with crystal hydrates with different morphologies: plate crystals (portlandite), needle crystals (ettringite) and fine crystal aggregates (C–S–H gel).

TG-TDG-DTA

The results from the thermal analysis for the studied samples at 28 and 120 days of curing are shown in Fig. 3 and Table 4, where four temperature ranges are specified. The mass losses in these ranges are as follows: I range—1.0–4.0 %, II range—0.7–1.3 %, III range—0.5–4.1 %, and IV range—2.3–29.1 %. Despite these low values, the evolution of hydration processes can be analysed by reducing the amount of portlandite (bonded water in portlandite) and the increase of water included

Table 3 Results from XRD analysis of the samples

No	Samples	Relict minerals	New formed minerals
1.	A28, A120	Quarz, SiO_2	Thaumasite, $Ca_3Si(SO_4)_2(OH)_6{\cdot}12H_2O$
		Belite (C_2S), β-Ca_2SiO_4	Portlandite, $Ca(OH)_2$
		Plagioclase,	Hemicarboaluminate,
		$(Na, Ca)Al(Si,Al)_3O_8$	$Ca_4Al_2(CO_3)_{0.5}(OH)_{12}{\cdot}5.5H_2O$ (A120 only)
			Ettringite, $Ca_6Al_2(SO_4)_3(OH)_{12}{\cdot}26H_2O$
2.	B28, B120	Dolomite, $CaMg(CO_3)_2$	Portlandite, $Ca(OH)_2$
		Mg-rich Calcite, $CaCO_3$	Ettringite, $Ca_6Al_2(SO_4)_3(OH)_{12}{\cdot}26H_2O$
		Belite (C_2S), β-Ca_2SiO_4	Hemicarboaluminate, $Ca_4Al_2(CO_3)_{0.5}(OH)_{12}{\cdot}5.5H_2O$ (B28 only)
		Plagioclase,	Monocarboaluminate, $Ca_4Al_2(CO_3)(OH)_{12}{\cdot}5H_2O$ (B120 only)
		$(Na, Ca)Al(Si,Al)_3O_8$	Hillebrandite, $CaSiO_3{\cdot}Ca(OH)_2$
			Xonotlite—$5CaO{\cdot}6SiO_2{\cdot}Ca(OH)_2$ (B28 only)
3.	C28, C120	Dolomite, $CaMg(CO_3)_2$	Portlandite, $Ca(OH)_2$
		Mg-rich Calcite, $CaCO_3$	Ettringite, $Ca_6Al_2(SO_4)_3(OH)_{12}{\cdot}26H_2O$
		Belite (C_2S), β-Ca_2SiO_4	Hemicarboaluminate, $Ca_4Al_2(CO_3)_{0.5}(OH)_{12}{\cdot}5.5H_2O$ (C28 only)
		Plagioclase,	Monocarboaluminate, $Ca_4Al_2(CO_3)(OH)_{12}{\cdot}5H_2O$ (C120 only)
		$(Na, Ca)Al(Si, Al)_3O_8$	Hillebrandite, $CaSiO_3{\cdot}Ca(OH)_2$ (C28 only)
			Xonotlite—$5CaO{\cdot}6SiO_2{\cdot}Ca(OH)_2$ (C28 only)

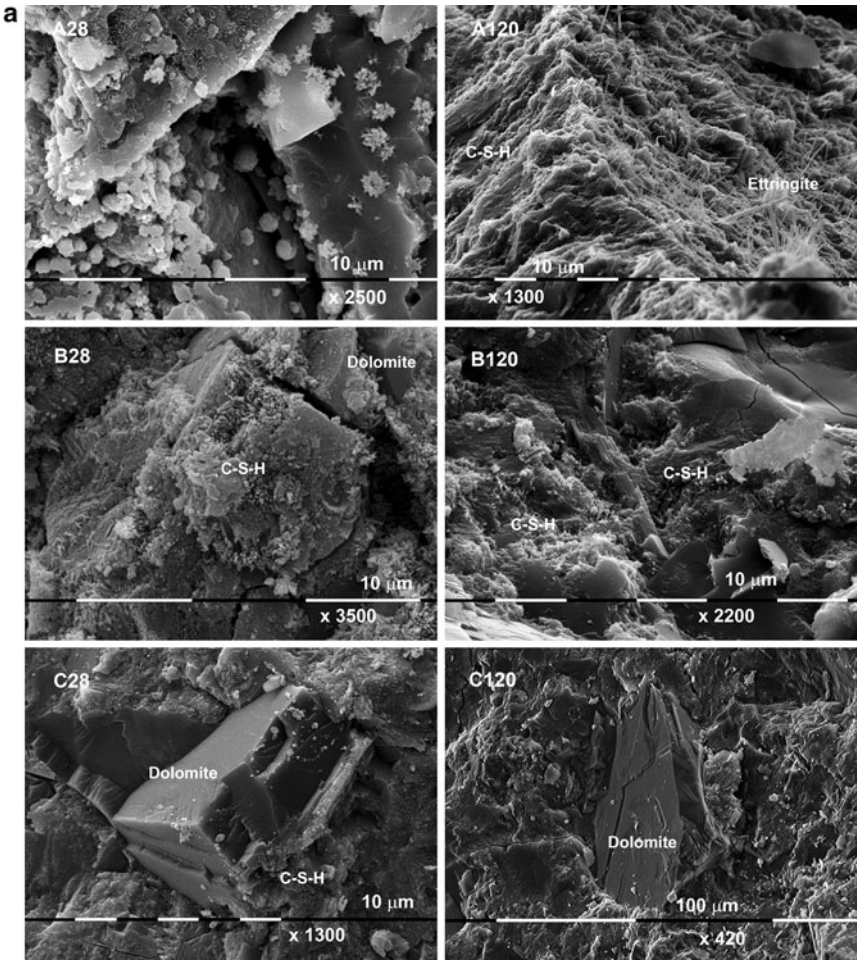

Fig. 2 **a** SEM micrographs of surface structures of samples A, B and C (28 and 120 days of water curing). **b** SEM micrographs of crystal hydrated phase of samples A, B and C (28 and 120 days of water curing)

Fig. 2 continued

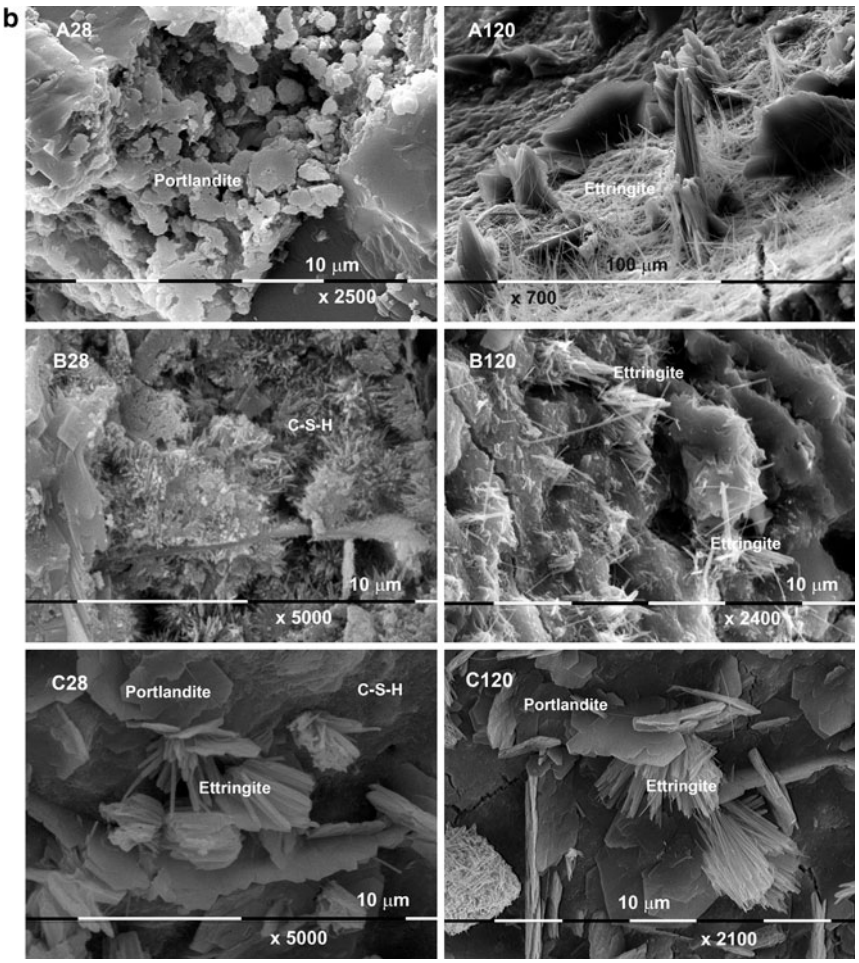

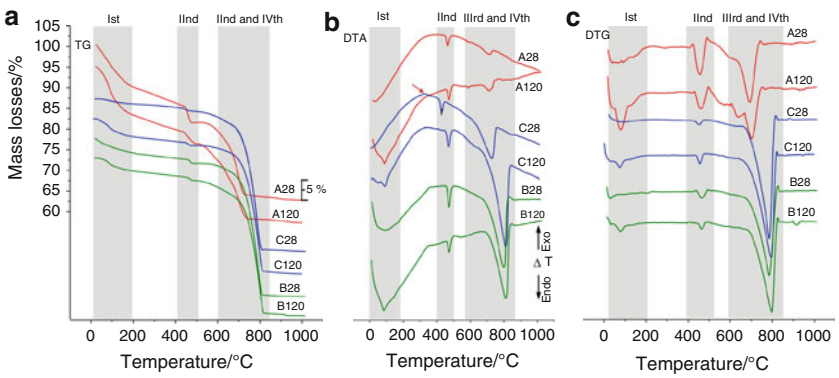

Fig. 3 Thermal decomposition of samples A, B and C (28 and 120 days of water curing): **a** TG curves; **b** DTA curves; **c** DTG curves

in the structure of C–S–H phases (Table 4). Moreover, based on the obtained data, the effects of water-to-cement ratio, water-to-powder ratio, dolomitic marble and HRWR on the structure of mortars may be investigated (Fig. 3a–c).

The data analysis of sample A show that prolonged curing in water increases the total mass losses from 6.60 % (A28) to 9.14 % (A120), caused by increased losses of water in the I and III ranges and decarbonization in the IV range. The mass losses due to dehydration of water in the II and III ranges are the smallest, and the ratio between the mass losses of portlandite to C–S–H phase in samples A28 and A120 is close to 1:1 (Table 4).

The use of dolomitic marble instead of sand in the mortars slightly increased the amount of the water bonded in portlandite in samples B28 and C28, but prolonged

Table 4 Temperatures of thermal decomposition ($T_{infl.}$) and mass losses of the samples

Region	I range		II range		III range		IV range		Total mass loses/%
	40–200 °C		420–470 °C		520–700 °C		700–800 °C		
Process	Dehydratation		Decomposition of $Ca(OH)_2$		Decomposition of C–S–H		Decarbonization of $MgCa(CO_3)_2$		
Sample	$T_{infl.}$/°C	Mass losses/%	$T_{infl.}$/°C	Mass losses/%	$T_{infl.}$/°C	Mass losses/%	$T_{infl.}$/°C	Mass losses/%	
A28	49.6 100.7 147.1	1.73	460.3	0.73	607.2	0.68	695.7	2.29	6.60
A120	43.0 87.2 141.7	2.74	467.9	0.66	577.7	1.08	703.5	3.34	9.14
B28	35.0 85.0 198.0	3.69	466.1	1.07	602.7	2.18	782.5	28.88	37.67
B120	40.5 86.7 143.7	2.85	469.2	0.97	591.5	4.07	788.3	27.64	37.63
C28	38.7 81.5 137.0	1.79	450.7	0.90	592.8	3.10	786.0	30.00	36.56
C120	41.0 88.1 139.8	4.11	464.2	0.82	593.7	1.41	798.6	29.12	37.71

hydration reverses this trend. The amount of water involved in the structure of C–S–H phases increases from 0.68 to 2.18 % in sample B28 (more than twice) and from 1.08 to 4.07 % in sample B120 (almost four times).

Prolonged hydration of sample C decreases the mass losses in III range (decomposition of C–S–H) from 3.10 % (C28) to 1.41 % (C120) (Table 4). This fact may be explained by reduction of pore space (Table 2), which is necessary for the growth of new C C–S–H phases, and the presence of HRWR admixture. This character of the structure confirms the results of XRD analysis, which identifies the highest diversity of the C–S–H phases in B120. The low contents of C–S–H phases in samples C are due to the very low water-to-cement and water-to-powder ratio (Table 1). These ratios plus the presence of polycarboxylate-based admixture allow for the formation of very dense structure, where the angular particles of aggregate are interlocked. The thermal 'traces' of HRWR admixture are registered in the DTA-curve of sample C28 (Fig. 3b)—broad exothermic low-intensity peak in the range of 420–470 °C.

The decomposition of carbonate-containing phases (IV range, Fig. 3a–c, Table 4) [17–19] of samples B and C is performed at higher temperatures, compared to samples A. The use of dolomitic marble as aggregate slightly increases the temperature of decarbonization with benefit of the samples C. The most accurate explanation of this fact is the formation of dense structure, which effect is reflected in the results of any physical analyses.

Conclusions

The structures of the two types of white cement high workability mortars with relatively high content of marble powder containing fine particles are investigated. The comparison with cement–sand mortars shows that high contents of fine particles make the structure denser, even prone to self-desiccation. The formed structure has open porosity, which allows for water transport with slow continuous hydration with formation of variety of products and the growth of crystals.

The use of polycarboxylate admixture allows decreasing the amount of water and improving the dispersion of the fine particles; thus, the hardened mortars reach their maximum compressive strengths, limited by the strength of the marble aggregates. Both the mass losses of dehydration (crystallization and structural water) and temperature of

decomposition of carbonate-containing phases increase, bringing out additional evidence for dense and strong structure of the studied mortars with high content of marble powder.

References

1. Lea's Chemistry of Cement and Concrete (Editor P.C. Hewlett). 4th Ed., Butterworth-Heinemann; 2004. p. 1092.
2. Hamad BS. Investigations of chemical and physical properties of white cement concrete. Adv Cem Based Mater. 1995;2:161–7.
3. Ling T-C, Poon C-S. Properties of architectural mortar prepared with recycled glass with different particle sizes. Mater Des. 2011;32:2675–84.
4. Perez-Rodriguez JL, Duran A, Perez-Maqueda LA. Thermal study of unaltered and altered dolomitic rock samples from ancient monuments The case of Villarcayo de Merindad de Castilla la Vieja (Burgos, Spain). J Therm Anal Calorim. 2011; 104:467–74.
5. Aïtcin P-C. Binders for durable and sustainable concrete. London: Spon Press; 2007. p. 528.
6. Aïtcin P-C, Mindess S. Mindess, sustainability of concrete. New York: Spon Press; 2011. p. 328.
7. De Schutter G, Bartos PJM, Domone P, Gibbs J. Self-compacting concrete. Caithness: Whittles Publishing; 2008. p. 288.
8. Duran A, Perez-Maqueda LA, Poyato J, Perez-Rodriguez JL. A thermal study approach to roman age wall painting mortars. J Therm Anal Calorim. 2010;99:803–9.
9. Self Compacting Concrete (Editor A. Loukili), Wiley; 2011. p. 288.
10. EN 196-1:2006, Methods of testing cement—Part 1: determination of strength.
11. Stoyanov V. Investigation of properties of decorative mortars based on design of experiments In: Proceedings of International Conference on Civil Engineering Design and Construction. (Eurocodes—Science and Practice) DCB 2010, September 09–11, 2010, Varna, Bulgaria, 463–470 (in Bulgarian).
12. ASTM C642-06 Standard test method for density, absorption, and voids in hardened concrete; 2006.
13. Matschei T, Lothenbach B, Glasser FP. The role of calcium carbonate in cement hydration. Cem Concr Res. 2007;37:551–8.
14. Aguilera J, Martınez-Ramırez S, Pajares-Colomo I, Blanco-Varela MT. Formation of thaumasite in carbonated mortars. Cement Concr Compos. 2003;25:991–6.
15. Taylor HFW. Cement chemistry. 2nd ed. London: Thomas Telford Publishing; 1997.
16. Barnett SJ. CD Adam, ARW Jackson, Solid solutions between ettringite, $Ca_6Al_2(SO_4)_3(OH)_{12}.26H_2O$, and thaumasite, $Ca_3Si-SO_4CO_3(OH)_6.12H_2O$, J. J Mater Sci. 2000;35:4109–14.
17. Pavlidou E. Systematic analysis of natural pozzolans from Greece suitable for repair mortars, J Therm Anal Calorim. doi: 10.1007/s10973-011-2039-y.
18. Federico LM, Chidiac SE, Raki L. Reactivity of cement mixtures containing waste glass using thermal analysis. J Therm Anal Calorim. 2011;104(3):849–58.
19. Goñi S, Puertas Fr, Hernández MS, Palacios M, Guerrero A, Dolado JS, Zanga Br, Baroni F. Quantitative study of hydration of C3S and C2S by thermal analysis evolution and composition of C–S–H gels formed. J Therm Anal Calorim. 2010;102:965–73.